Proceedings World Geothermal Congress 2020+1
Reykjavik, Iceland, April - October 2021

A Surface Conductive Heat Flux Tool to Delineate Geothermal Reservoirs

Graeme R. Beardsmore

PO Box 251, South Yarra, VIC 3141, AUSTRALIA

graeme.beardsmore@hotdryrocks.com

Keywords: Heat flow, exploration, geophysics, reservoir characterization, emerging technology

ABSTRACT

Surface conductive heat flux theoretically provides the most direct evidence of the existence, location and extent of a buried concentration of geothermal energy because it is governed by the same potential field mathematics that describes gravity, magnetics and electromagnetic geophysical techniques. Geothermal reservoirs theoretically generate measurable surface heat flux anomalies. This fact underpins the use of 'heat flow wells' to confirm a heat source before appraisal drilling for deep hydrothermal systems. Heat flow wells are, however, expensive to drill, which precludes their use as a routine exploration tool to detect and delineate geothermal reservoirs. This paper provides an update on the development of one meter long probes that can be deployed at relatively little cost across an entire geothermal prospect area, and which measure conductive surface heat flux. Field trials in Australia and Mexico (and planned for New Zealand) have demonstrated the tool's ability to quantify conductive surface heat flux to an accuracy and precision of about ± 50 mW/m^2. Clear variations in surface heat flux on the order of W/m^2 have been delineated over known hydrothermal systems, demonstrating the potential to map the distribution of subsurface heat at regional scale. The tool shows great promise to improve exploration efficiency by identifying areas with high concentrations of sub-surface heat prior to appraisal drilling.

1. INTRODUCTION

1.1 Geothermal energy exploration

The interior of the Earth is hot relative to the Earth's surface. That is, the Earth contains a lot of thermal energy (heat) from primordial sources and ongoing radioactive decay. The primary goal of geothermal energy exploration is to find geothermal 'reservoirs'—volumes of rock within which heat has accumulated in the subsurface in such a concentration that it can be economically extracted to the surface through production bores. But many geothermal exploration tools do not target heat; they instead target the indirect effects of subsurface heat such as changes in electrical properties of rocks, subtle differences in fluid density, or increased chemical solubility. These indirect methods are restricted in their ability to delineate the precise location, depth, magnitude and/or time of the associated geothermal reservoir. Anomalies identified with indirect methods can be relics of historical, but since dissipated, geothermal reservoirs, or could even be generated by factors other than heat.

The First and Second Laws of Thermodynamics can guide a geothermal energy exploration strategy. Those laws govern how heat moves through the subsurface. The First Law of Thermodynamics ('conservation of energy') dictates that all heat within the Earth must be conserved; heat is either converted to other forms of energy—for example by driving endothermic reactions, phase changes, tectonic plate motions and fluid convection—or else the heat simply flows from one location to another. The Second Law of Thermodynamics ('increasing entropy') dictates that heat will always spontaneously flow from higher to lower temperatures.

Of the commonly applied geothermal exploration tools, only conductive heat flux estimates from 'heat flow wells' (e.g. Allis *et al*., 2017), convective heat flux estimates from methods such as calorimetry (e.g. Hochstein and Bromley, 2005), and radiative heat flux estimates from thermal infrared imagery (e.g. Mia *et al.*, 2012; Vaughan *et al*., 2012) exploit thermodynamic principles to quantify parts of the subsurface 'heat budget'. Heat flux through the shallow parts of the Earth is entirely by convection and conduction, while radiation and convection account for the further dispersion of the heat into the atmosphere and beyond. The contribution of conduction to subsurface heat flux is often overlooked in geothermal exploration, but not always. Reeves *et al*. (2018), for example, attempted to quantify both conductive and convective heat flux for the Waimangu Geothermal Valley in New Zealand, and Lindsey *et al*. (2019) conducted a similar exercise for parts of Yellowstone National Park.

Each of the existing exploration tools directly targeting heat have their limitations for locating and delineating geothermal reservoirs. Radiative flux techniques can only sense heat flux >> 1 W/m^2. Both convective and radiative heat flux measurements can only be made on springs, fumaroles and steaming ground where the land surface is significantly hotter than surrounding areas. Such features imply that fluids have transported heat from an existing geothermal reservoir to the surface, but provide no indication of the vertical or lateral distance travelled by the fluids. Such measurements, therefore, might help quantify the total heat content of the reservoir, but not its location, depth or extent. Furthermore, not all geothermal reservoirs are associated with surface manifestations. By definition, 'blind' geothermal systems do not discharge any heat to the surface by convection, and land surface temperature above blind systems is usually indistinguishable from surrounding areas within the resolution of radiative heat flux methods.

Conduction is the overwhelmingly dominant mode of heat flux above blind geothermal systems, and conduction also accounts for a significant portion of heat flux from geothermal systems with associated surface manifestations. Lindsey *et al*. (2019), for example, estimated that 41% of the total heat flux from the geothermal system feeding the Bravo Hot Springs in Yellowstone National Park is conductive. Quantifying and mapping both the conductive and convective components of surface heat flux around geothermal systems would provide the most direct evidence of the size and location of a geothermal reservoir prior to drilling. But measuring conductive heat flux in heat flow wells is prohibitively expensive as a routine exploration strategy, so heat flow wells are only drilled to confirm a thermal anomaly prior to deep appraisal drilling after indirect surface exploration. When coupled with existing methods of measuring convective surface heat flux, a cost effective tool to measure conductive heat flux at the Earth's surface could significantly increase the success rate of geothermal exploration by completely quantifying the thermal budget of a geothermal system, confirming the existence and location of heat anomalies prior to surface drilling. This paper describes such a tool.

1.2 Surface conductive heat flux

When considered together, the two Laws of Thermodynamics tell us that the Earth's internal heat must, on average, continuously flow through the Earth's surface via the mechanisms of conduction and convection. Conduction accounts for a significant (often entire) portion of the heat flux emanating from every geothermal reservoir, even if the reservoir itself is part of a convection system (e.g. Lindsey *et al*., 2019). Furthermore, heat conduction obeys the same potential field laws as gravity (Beardsmore, 2016). As with gravity anomalies, conductive heat flux anomalies observed at the Earth's surface lie *directly above the heat source causing the anomaly*! Infrared thermal imaging cameras exploit this principle by detecting the radiative heat flux from surfaces through which heat is conducting from underlying sources (Figure 1). Conductive heat flux measured and mapped at the Earth's surface could, therefore, directly delineate the location of an underlying geothermal reservoir. By further analogy with gravity, conductive surface heat flux maps could enable quantitative interpretation of buried heat sources. In other words, a surface conductive heat flux map could potentially reveal the extent, depth and temperature of a geothermal reservoir prior to significant drilling.

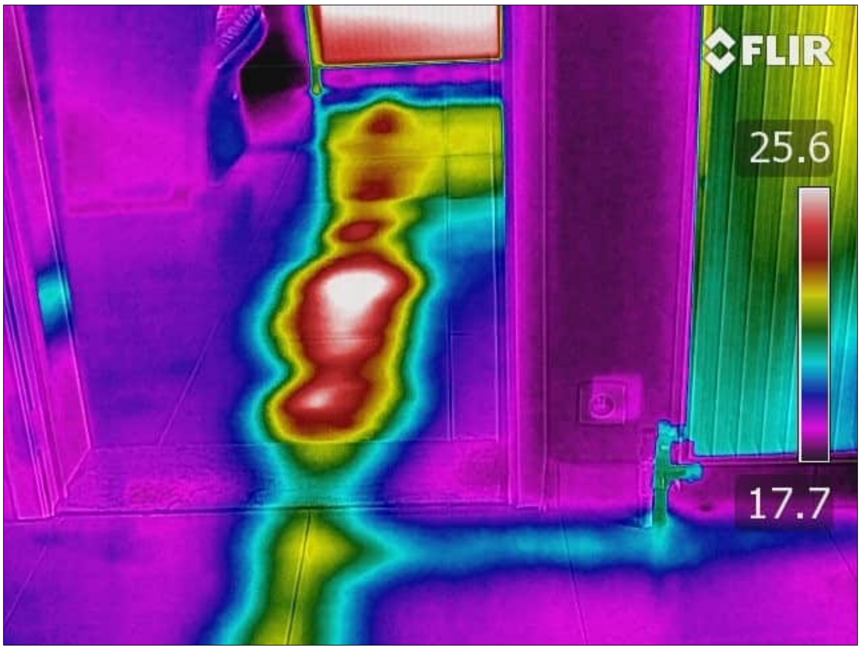

Figure 1: A heat source detected beneath a solid floor by a thermal infrared camera. Heat conducts through the floor to the surface, from where it radiates and convects into the air. Directly mapping the conductive heat flux through the surface of the floor could fully constrain the location, depth and magnitude of the heat source. Source: https://www.cibor.be/en/cibor-scores-infrared-leak-detection-camera-inspection-piping/

While conductive heat flux is undoubtedly a key indicator of the geothermal prospectivity of an area, it is very challenging to determine its value at the Earth's surface. Conductive heat flux is the amount of thermal energy passing through a unit surface area per unit of time; watts per square meter (W/m^2) in S.I. units. In practice, conductive heat flux is calculated as the product of temperature gradient (kelvin per meter, K/m) and thermal conductivity (watts per meter per kelvin; W/mK). The temperature gradient due to heat flux through continental crust is typically on the order of 0.025–0.030 K/m (25–30°C/km; Goldstein *et al*., 2011). Conventional instruments and methods can only quantify a gradient of this magnitude over borehole intervals of tens of meters, but Beardsmore and Antriasian (2015) described the design and calibration of bespoke sensors able to do it over an interval of just one meter. At the time of writing, one meter remains the minimum practical depth interval over which typical continental geothermal gradient can be quantified with reasonably accuracy (better than ± 3°C/km).

1.3 Conductive heat flux above geothermal reservoirs

An exploration tool must be sensitive and accurate enough to detect and quantify the target of interest. A simple scenario can be used to estimate the magnitude of surface heat flux generated by a potentially commercial geothermal reservoir. Consider a hypothetical 250°C geothermal reservoir lying at a depth of 1,500 m beneath an impermeable volcanoclastic succession of rocks in a location where the average surface temperature is 25°C. The average thermal gradient down to the reservoir is (250 - 25) / 1,500 = 0.15 K/m, or 150°C/km. Assuming a thermal conductivity of 2.5 W/mK for volcanoclastic material, and recalling that conductive heat flux is the product of thermal gradient and thermal conductivity, surface heat flux above the hypothetical reservoir is 0.15 x 2.5 = 0.375 W/m^2, or 375 mW/m^2. This prediction is supported by published examples of near surface conductive heat flux above known economic geothermal reservoirs. Magro *et al*. (2009) modelled the surface conductive heat flux over the Larderello Geothermal Field in Italy, based on thermal conductivity and borehole temperature measurements. Their results indicate that the 200–260°C reservoir at depths of 500–1200 m (Minissale, 1991) generates a regional conductive heat flux of about 300 mW/m², peaking around 800 mW/m² above shallow reservoir pockets (Figure 2a) . Allis *et al*. (2017) delineated surface conductive heat flux exceeding 400 mW/m² (Figure 2b) above the 175°C Cove Fort geothermal reservoir in Utah, which lies at a depth of 1,600 m and feeds a 26 MW_e binary power plant (Sacerdoti, 2015). These hypothetical and real examples demonstrate that surface heat flux above economic geothermal reservoirs is typically many times greater than typical continental heat flux (~65 mW/m²; Pollack *et al*., 1993). But the magnitude of the conductive heat flux is far below the detection limits of radiative flux techniques (>> 1 W/m²).

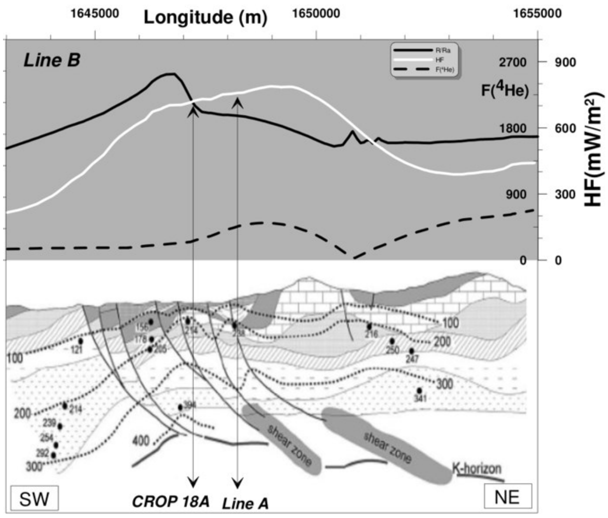

(a)

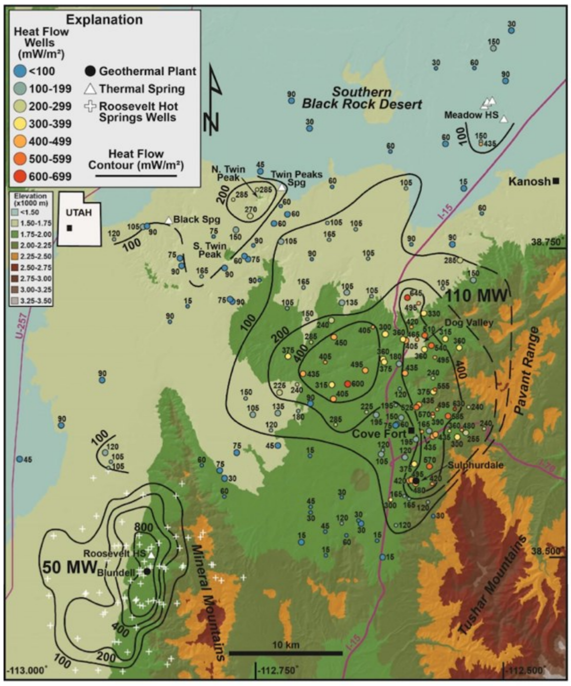

(b)

Figure 2: (a) Top chart, white line: Modelled conductive surface heat flux across the Larderello Geothermal Field, Italy (Magro *et al*., 2009.) The geothermal reservoir generates a surface heat flux anomaly of > 500 mW/m² above the regional trend, over a lateral distance of about 5 km. (b) Black contours: Estimated conductive surface heat flux around the Cove Fort geothermal field, Utah (Allis *et al*., 2017.) The geothermal reservoir generates a surface heat flux anomaly of > 300 mW/m² over tens of square kilometers.

2. THE HEAT NEEDLE

Beardsmore (2012) and Beardsmore and Antriasian (2015) described the concept, construction and calibration of Heat Needles to achieve absolute measurement of ground temperature with an accuracy on the order of ± 3.0 mK and precision on the order of ± 0.3 mK, and to conduct *in situ* measurements of ground thermal conductivity. Beardsmore *et al*. (2017) reported on a field trial of Heat Needles in the Los Azufres Geothermal Region of Mexico, during which variations in surface conductive heat flux were measured relative to a baseline site to a precision of ± 500 mW/m² (Figure 3). That paper concluded that "advances in data processing should lead to progressively greater precision in the interpretation of surface heat flow relative to 'background' sites."

The concept underpinning the Heat Needle is that the conductive heat flux measured at the Earth's surface at any given time, $Q_m(t)$, is the sum of the constant geothermal heat flux from below, Q_g, and the varying heat flux from the diffusion of the varying temperature of the Earth's surface induced by solar and meteorological processes, $Q_v(t)$:

$$Q_m(t) = Q_g + Q_v(t) \tag{1}$$

Where subscripts m, g and v refer to 'measured', 'geothermal' and 'varying', respectively. Put another way, the constant geothermal heat flux can be calculated by subtracting the variable component of surface heat flux from the measured signal:

$$Q_g = Q_m(t) - Q_v(t) \tag{2}$$

Heat Needles measure $Q_m(t)$ with high precision and accuracy, so the challenge is to maximize the precision and accuracy of $Q_v(t)$. One approach is to forward model variations in near surface heat flux induced by real fluctuations in surface temperature through time at each survey site. In line with this approach, the following sections briefly describe three significant improvements in the data processing algorithm since the Beardsmore *et al*. (2017) paper. These three improvements have, in some cases, increased the precision of Q_g determinations ten-fold to ± 50 mW/m² (Figure 4).

(1) Objective quantification of thermal diffusivity;
(2) Reconstruction of surface temperature history prior to the Heat Needle survey, and;
(3) Analytical forward modelling of the downward diffusion of the inferred surface temperature history.

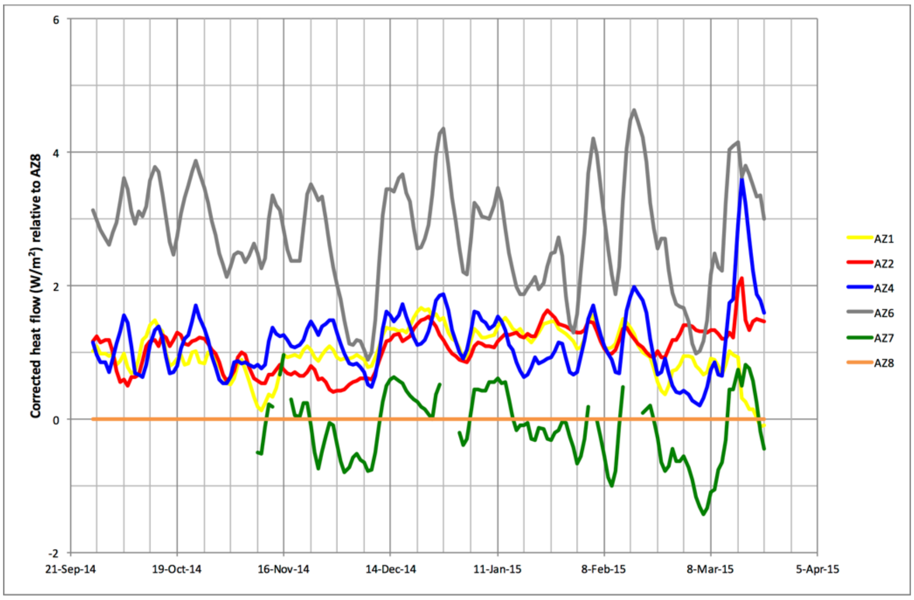

Figure 3: Inferred conductive geothermal surface heat flux, Q_g, as a function of time at five sites in the Los Azufres Geothermal Region, relative to background site AZ8, as reported by Beardsmore *et al*. (2017).

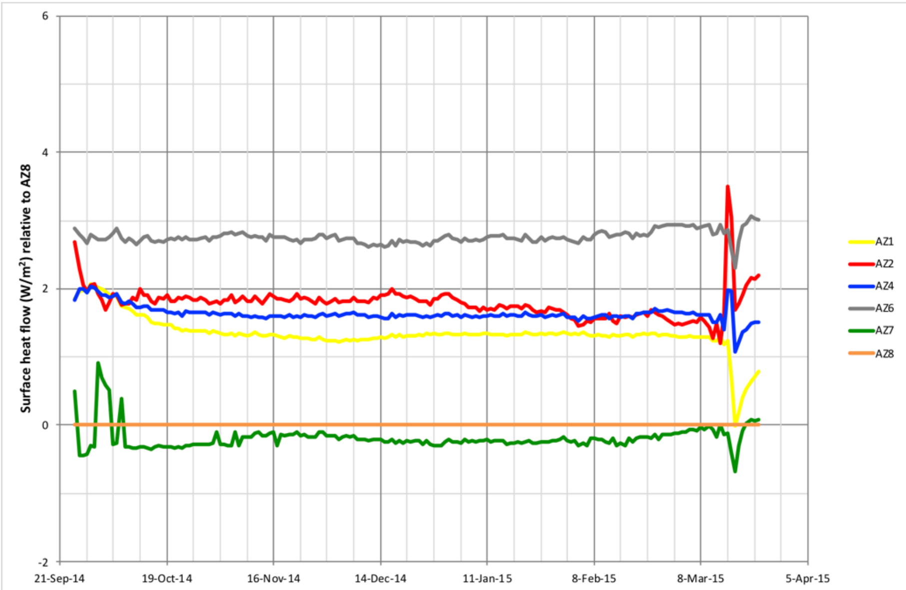

Figure 4: Inferred conductive geothermal surface heat flux, Q_g, as a function of time at five sites in the Los Azufres Geothermal Region, relative to background site AZ8, with improved processing of the datasets from Figure 3.

2.1 Quantification of thermal diffusivity

Conductive heat flux is the product of thermal gradient and thermal conductivity, so one of the key objectives is to quantify the impact that varying surface temperature has on near-surface thermal gradient. This is directly related to the rate at which isothermal surfaces diffuse through the ground, which is controlled purely by the thermal diffusivity of the ground. Thermal diffusivity is challenging to measure *in situ*, but Beardsmore *et al*. (2020) described a method to calculate the magnitude and uncertainty of thermal diffusivity from Heat Needle time–temperature records. Each Heat Needle measures temperature simultaneously at seven depths (surface plus six subsurface depths) at discrete time intervals (typically every 15 minutes) for periods of weeks to months. Converting the time-series records into the frequency domain using discrete Fourier transforms allows the direct comparison of amplitudes and phases of significant frequency components at different depths. Meteorological events induce a wide spectrum of thermal signal frequencies at the surface, which each diffuse into the shallow subsurface. The phase offset and decay in amplitude observed between shallower and deeper sensors for any given frequency are both functions of the average thermal diffusivity of the soil between the two sensors (e.g. Carslaw and Jaeger, 1959, Section 2.6). The magnitude and uncertainty of thermal diffusivity can be inferred by evaluating the apparent thermal diffusivity affecting each discrete frequency band over the full spectrum (Figure 5a). A discrete thermal diffusivity depth profile is obtained from surface to 1.1 m depth by calculating the diffusivity between successively deeper sensors (Figure 5b). In most cases, interval thermal diffusivity can be calculated to a precision better than ± 5%. Thermal diffusivity can also be calculated between the surface and any subsurface sensor using the same method.

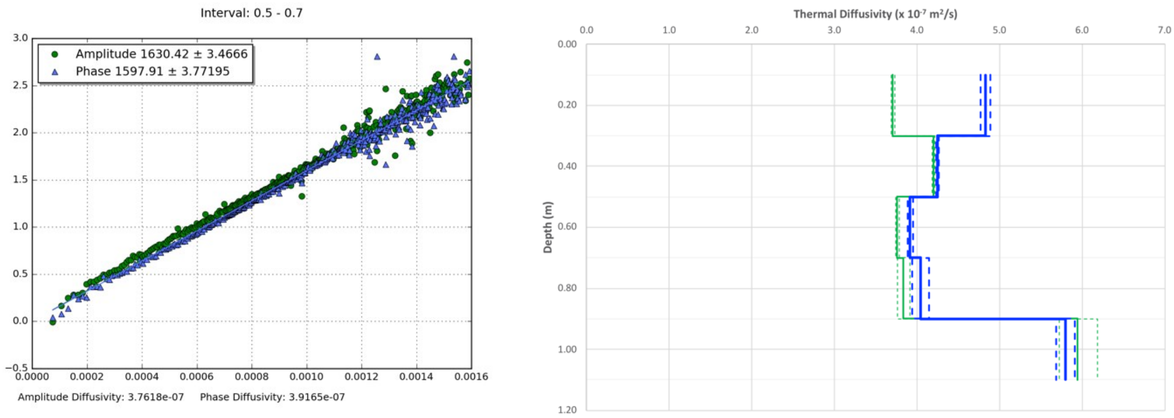

(a) (b)

Figure 5: (a) Chart of amplitude decay coefficients (green circles) and phase shift (radians; blue triangles) versus a variable related to signal frequency for all frequency bands recorded by Heat Needle sensors at 50 cm and 70 cm depth over a nine-month period at a site in South Australia. Thermal diffusivity is calculated for that depth interval from the slope and uncertainty of the resulting line. (b) Vertical profile of thermal diffusivity (with dashed uncertainty bands) calculated from phase (blue) and amplitude (green) information for each sensor depth interval. Refer to Beardsmore *et al*. (2020) for a detailed description of the methodology.

2.2 Reconstruction of surface temperature history

The thermal gradient in the top meter of the Earth is strongly impacted by the diurnal and annual solar heating cycles. In winter, the average land surface temperature is lower than the long term mean, which produces a large transient increase in near-surface thermal gradient. The opposite is true in summer, when the average land surface temperature is higher than the long-term mean and the near-surface gradient is temporarily greatly reduced. The magnitude of the effect can be modelled for any given scenario. The principle of superposition dictates that the impacts of sequential temperature cycles are cumulative. This means that the surface temperature cycle over any given year can affect the near-surface thermal regime for a significant time into the future, superimposed onto the thermal impacts of prior and subsequent years.

For example, consider a typical location exposed to a single sinusoidal annual temperature cycle with an amplitude of ± 10°C, beginning and ending on the autumnal equinox (Figure 6a). That single cycle affects both the temperature and thermal gradient of the shallow subsurface. The red line on Figure 6b shows the impact of that single cycle on the temperature of the ground between 0.1 m and 1.1 m depth at the immediate end of the cycle (i.e. at Time = 0.00 years on Figure 6a) for an assumed thermal diffusivity of 3 x 10^{-7} m^2/s; namely, an increase in temperature of between 2.0°C and 3.3°C relative to the annual mean temperature. Orange, yellow, green and blue lines on Figure 6b predict the exponential decay of the temperature spike over the following eight years. The end of the annual cycle also coincides with an elevation in thermal gradient of about 2,400°C/km in the top 1.1 m relative to the geothermal gradient we are aiming to detect. This increase in gradient also decays in magnitude over time, falling below 3°C/km (the practical limit of Heat Needle resolution) after about five years (Figure 6c).

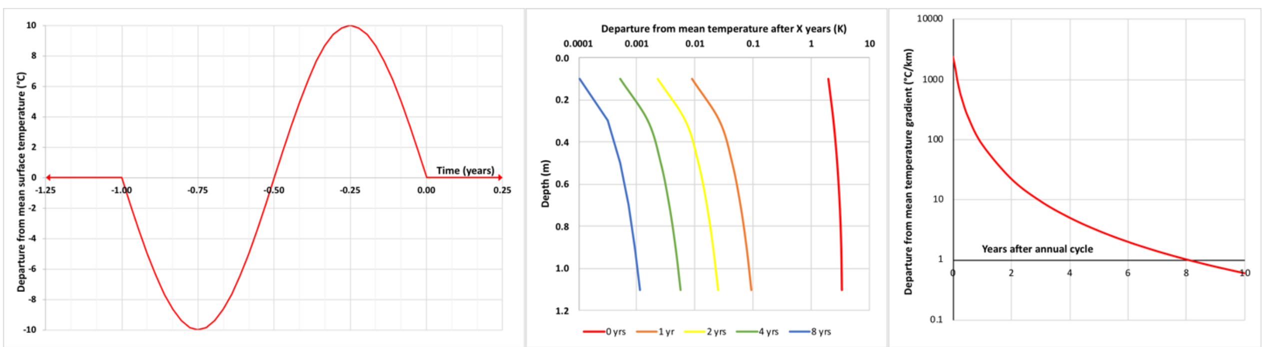

(a) (b) (c)

Figure 6: (a) Departure from mean surface temperature due to a single sinusoidal annual cycle beginning and ending on the autumnal equinox. (b) Effect on temperature between 0.1 m and 1.1 m depth due to diffusion of the annual surface cycle after 0 years (red), 1 year (orange), 2 years (yellow), 4 years (green) and 8 years (blue). (c) Effect on thermal gradient in the top 1.1 m of the ground due to diffusion of the annual surface cycle over time. See text for model details.

What this means in practice is that the thermal gradient (and, hence, conductive heat flux) in the top 1.1 m of the ground is overwhelmingly dominated by the downward diffusion of the surface temperature cycle experienced at the site over the preceding year, and that the previous five annual cycles might all significantly overprint a geothermal anomaly of interest (c.f. Figure 2). Heat Needles precisely record surface temperature during their deployment, but obviously do not record surface temperature *prior* to deployment. A means is required to estimate the surface temperature trajectory over a period of at least five years (and preferably longer) prior to the end of each Heat Needle deployment. That could be achieved by deploying each Heat Needle for a minimum of five years, but this would render it impractical as a routine exploration tool.

Land surface temperature is rarely measured directly, but other types of data can be closely correlated with land surface temperature. Local meteorological records of daily maximum and minimum air temperature, for example, often extend many years into the past. While air temperature is only one of the variables that affects land surface temperature (the other major influence being direct radiation), the two are closely correlated. Approximate mean daily air temperature (the average of maximum and minimum recorded air temperature) can be correlated with mean land surface temperature recorded by a Heat Needle on the same days (for example, the average of 96 consecutive surface sensor records at 15-minute intervals) to determine a relationship whereby historical mean daily land surface temperature can be inferred from historical air temperature records.

Proximal meteorological records are often unavailable at locations of interest for geothermal exploration. But MOD11A1.006 and MYD11A1.006 products can be obtained for free through the online Application for Extracting and Exploring Analysis Ready Samples (‘AppEEARS’; https://lpdaacsvc.cr.usgs.gov/appeears/) courtesy of the NASA EOSDIS Land Processes Distributed Active Archive Center (LP DAAC), USGS/Earth Resources Observation and Science (EROS) Center, Sioux Falls, South Dakota. These two products each provide an estimate of land surface temperature at one square kilometer resolution over most of the world’s continental surface for each cloud-free day and night since the early 2000s, derived from sensors on NASA’s Terra and Aqua satellites. The daily average surface temperature recorded by a Heat Needle at a precise location is generally well correlated with the night time temperature observed by the satellites over the corresponding 1 km^2 pixel (e.g. Figure 7).

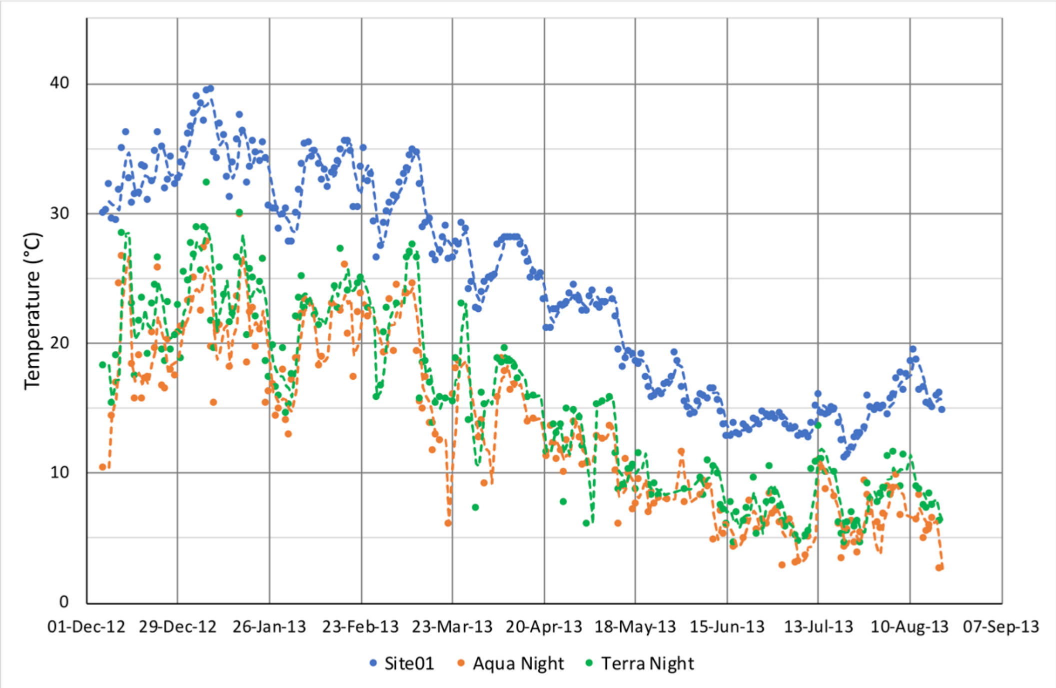

Figure 7: Night time land surface temperatures observed by Aqua (orange) and Terra (green) satellites, and daily average surface temperatures recorded by a Heat Needle (blue), at a site in South Australia over a nine-month period. In this case, the daily average temperatures recorded by the Heat Needle were about 10°C higher than the instantaneous night time temperatures observed by the satellites.

After determining a relationship between satellite and Heat Needle data through regression or other means, historical satellite data can be used to infer the likely surface temperature history at the Heat Needle site back to the beginning of the satellite records in the early 2000s (e.g. Figure 8). Even a correlation as rudimentary as a constant temperature offset between satellite and Heat Needle temperatures allows a basic reconstruction of the surface temperature history at the Heat Needle site. But there is enormous scope to apply more sophisticated regression algorithms (e.g. machine learning) to quantify and improve the confidence with which the surface temperature history is inferred.

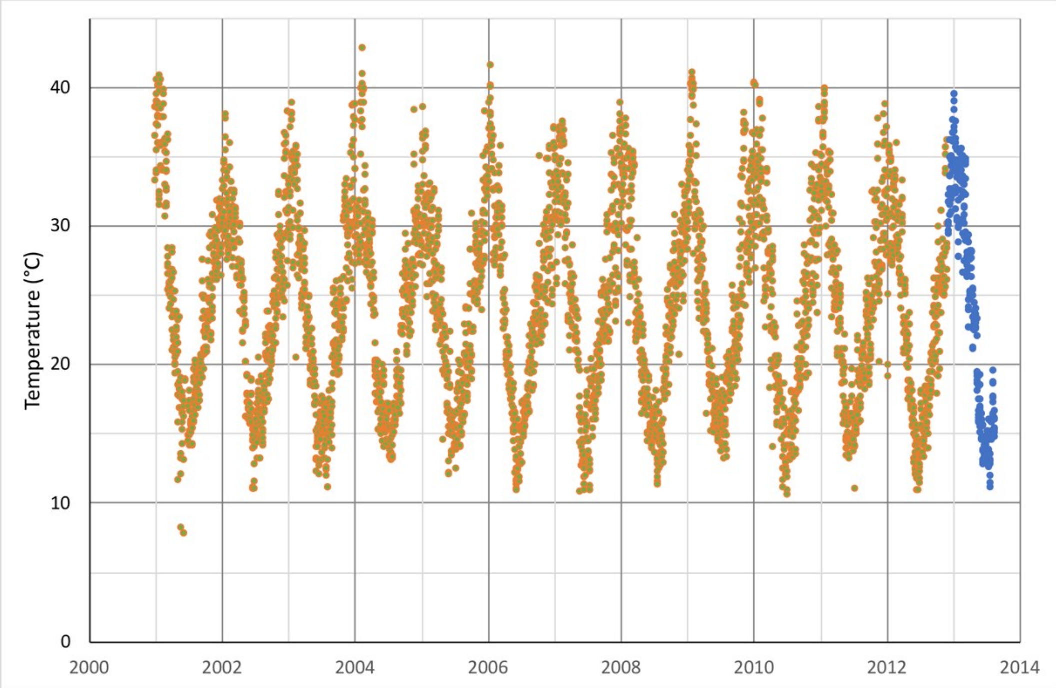

Figure 8: Reconstruction of the average daily surface temperature at the Heat Needle site in Figure 7 (orange and green circles) from the mean of both Aqua and Terra night time temperatures. The reconstructed history extends the surface temperature record almost 12 years into the past prior to the Heat Needle survey period (blue).

2.3 Forward modelling of heat diffusion

The third key advance in Heat Needle data processing since Beardsmore *et al*. (2017) has come from incorporating analytical forward model calculations of heat diffusion. There are analytical solutions for the thermal diffusion of any given surface temperature record (c.f. Section 2.2) into a half space with a known thermal diffusivity structure (c.f. Section 2.1). One relatively simple approach is to calculate the impact on the long-term mean subsurface temperature due to every discrete change in daily surface temperature over the period of reconstructed historical surface temperature. Carslaw and Jaeger (1959; Section 2.5) gave the following solution:

$$T_{z,t} = T_0 \times erfc\left(z/\left(2\sqrt{\kappa t}\right)\right) \quad (3)$$

Where $T_{z,t}$ is the discrete impact on subsurface temperature at depth, z, and time, t, after an instantaneous change in surface temperature of T_0; κ is the bulk thermal diffusivity between the surface and depth, z; and *erfc*() is the complementary error function. The principle of superposition ensures that the impact of each discrete change in surface temperature over the full history can be summed to determine their collective effect on subsurface temperature.

This approach is implemented in practice by modelling the ground as an infinite half-space at an initial isothermal temperature equal to the average surface temperature over a period of at least five full annual cycles prior to the end of the Heat Needle record. Equation (3) is then applied sequentially to each day in the surface temperature record, where each value of T_0 is the difference between the surface temperature on a given day and the surface temperature on the preceding day. Computational complexity is unavoidable because the cumulative effect of the full surface temperature history must be calculated for each day *and* each sensor depth of each Heat Needle record. But once the transient temperature disturbance is quantified, a 'reduced temperature' record can be calculated for each sensor depth from the difference between the transient disturbance and the observed ground temperature over the same period. Constant residual temperatures define a constant thermal gradient (e.g. Figure 9) that can be multiplied by the measured thermal conductivity to reveal the conductive geothermal heat flux (e.g. Figure 10).

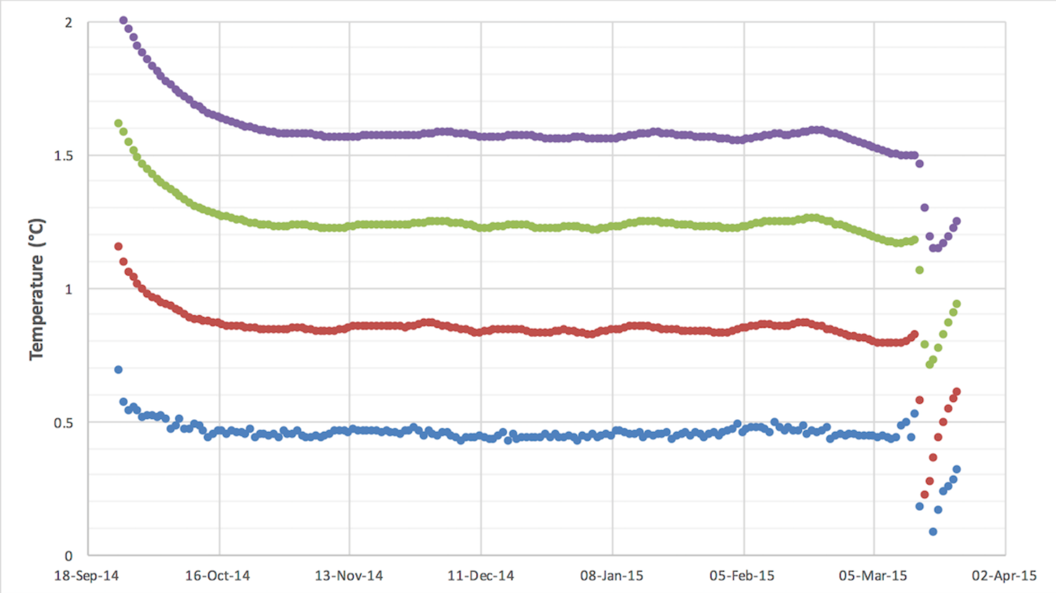

Figure 9: Reduced subsurface temperature calculated for 0.5 m (blue), 0.7 m (red), 0.9 m (green) and 1.1 m (purple) sensor depths over a six month period for the AZ4 site shown on Figure 4. The results indicate a relatively constant residual thermal gradient of about 1.9°C/m that can be attributed to geothermal heat flux.

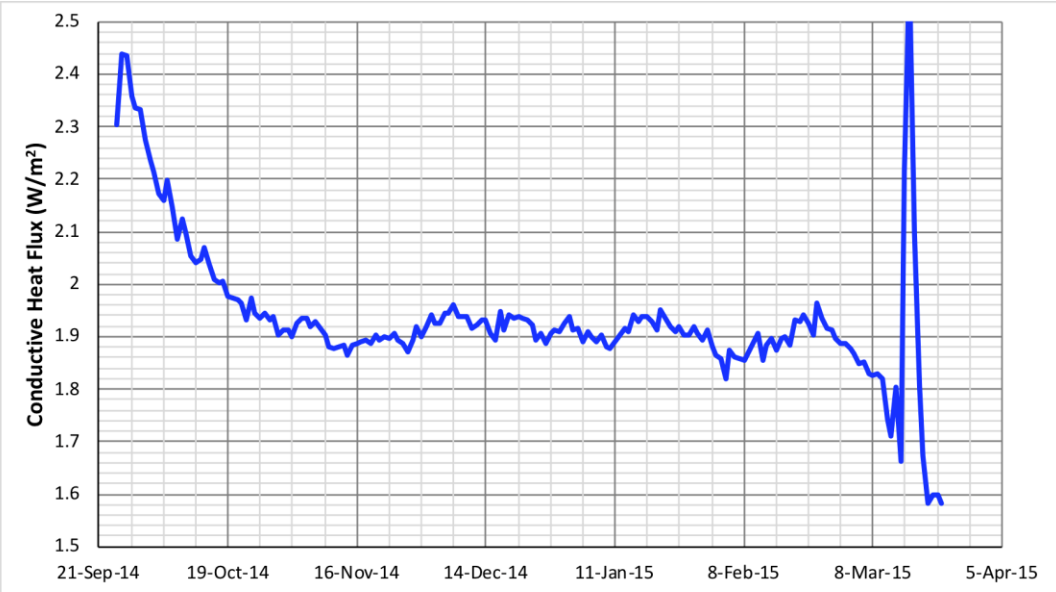

Figure 10: Inferred conductive heat flux through time for the AZ4 site shown on Figure 4.

Figure 10 suggests periods of apparent departure from constant conductive geothermal heat flux over both the initial and final weeks of the Heat Needle record. Like the annual cycle, meteorological temperature cycles with periods on the order of one week can impact the near surface ground temperature for up to five subsequent cycle-lengths. The initial period of 'equilibration', therefore, is likely due to inaccuracies in the average surface temperatures inferred from satellite records in the immediate days and weeks preceding the Heat Needle survey. Figure 9 suggests that the ground was, in fact, about 0.4°C warmer at 1.1 m depth than the forward model predicted at the start of the Heat Needle record.

The sharp disturbance to the reduced ground temperatures and conductive heat flux apparent in the last weeks of Figure 9 and Figure 10, respectively, coincided with a severe precipitation event. They probably reflect a departure from the assumption of pure conduction, constant thermal diffusivity, or both, as cold rain permeated into the ground. The four months of relatively constant (± 0.05 W/m^2) inferred heat flux in the middle of the record implies that minor precipitation likely has little impact on the results.

3. FURTHER REFINING THE ALGORITHM

Even with the rudimentary processing algorithms presented in this paper, the Heat Needle has demonstrated its ability to map regional variations in conductive heat flux to a precision better than ± 50 mW/m^2 with deployment periods of less than six months. That precision would easily delineate the thermal anomalies presented on the cross section and map reproduced on Figure 2, but at a fraction of the price of drilling the boreholes that provided the data for Figure 2. The 'disturbances' on Figure 10, however, illustrate that there remains considerable scope for refining the algorithm. Further improvements will likely come from:

(1) Improving the confidence of surface temperature history reconstructions;
(2) Incorporating time-varying thermal diffusivity and conductivity into the algorithm;
(3) Restructuring the algorithm into a probabilistic (e.g. Bayesian) framework.

3.1 Improving the confidence of surface temperature history reconstructions

Section 2.2 already anticipated this possibility. Machine learning tools, in particular, could be employed to discover subtle correlations between high-fidelity Heat Needle surface temperature measurements; a rich array of raw and processed data products from Aqua, Terra and other satellites; proximal meteorological records; digital elevation models; and any other data sets that might provide some constraint on surface temperature. The objective would be to accurately extend the Heat Needle records of daily average surface temperature at least five years into the past, and simultaneously determine an accurate 'long term mean' surface temperature. Ideally, such a process would define a 'probability distribution function' over the long-term mean surface temperature and the temperature on each day of the five-year history.

3.2 Incorporating time-varying thermal diffusivity into the algorithm

Equation (3) assumes that thermal diffusivity (κ) has a constant value through time. Charts such as those on Figure 5 are usually produced using the full record of data spanning the Heat Needle deployment period, and thus reveal the *average* thermal diffusivity over the full period. But thermal diffusivity can vary through time in response to physical factors such as changes in soil moisture. When the true diffusivity is higher than the assumed value, the subsurface responds to changes in surface temperature faster than the forward model predicts; and when the true diffusivity is lower than assumed, the subsurface response is slower than predicted. This is a possible source of 'noise' in the results produced by the current Heat Needle processing algorithm.

Beardsmore *et al*. (2020) demonstrated that temporal changes in thermal diffusivity can be detected and quantified through careful processing of Heat Needle data. The process can determine thermal diffusivity as a function of time with a maximum temporal resolution of about three weeks. The main challenge is to incorporate time-varying thermal diffusivity into the forward modelling algorithm. Predicting the diffusion of an irregularly-varying surface temperature signal into a medium with irregularly-varying thermal diffusivity poses a tractable but non-trivial computational problem. Work continues on this front.

3.3 Restructuring the algorithm into a probabilistic (e.g. Bayesian) framework

The current algorithm is deterministic. Single values of inherently uncertain parameters must be assumed in order to produce a single estimate of geothermal heat flux. The uncertainty of the outcome cannot currently be quantified. It is a complex function of uncertainties introduced into the process via the adopted values of thermal diffusivity and thermal conductivity, the inherent accuracy of the Heat Needle temperature measurements, the reconstructed surface temperature history, the discretization of temperature and depth, the simplified 'infinite half space' model, assumptions of stationary thermal properties, and the ever-present possibility of human error at various stages of the process. Restructuring the entire process into a Bayesian framework would allow all the uncertainties to be explicitly acknowledged and accounted for while generating a probabilistic outcome. The immediate value would be in quantifying the uncertainty of a derived value of geothermal heat flux. Additional value would come from identifying the primary sources of uncertainty, which could inform future directions of refinement.

4. CONCLUDING REMARKS

Both potential field theory and published studies demonstrate that commercial geothermal reservoirs are associated with significant surface conductive heat flux anomalies. The principle underpins the judicious (because of their significant cost!) use of 'heat flow wells' to confirm the presence of heat sources before deep appraisal drilling. If surface conductive heat flux could be routinely mapped, the maps could be interpreted to detect, delineate and quantify the temperature and depth of underlying hydrothermal reservoirs. Over the past decade, the Heat Needle has developed from a theoretical concept to a real device with a demonstrated ability to measure conductive surface heat flux with a resolution of ± 50 mW/m^2. This is sufficient to produce heat flux maps at a fraction of the cost of even a single 'heat flow well.' The Heat Needle offers the promise of routine heat flow mapping over prospective geothermal areas to identify and characterize heat sources, and specific locations above those heat sources, worthy of drilling. At the time of writing (December 2020), planning is underway to commence survey-scale trials of Heat Needles at one location in South Australia in the first half of 2021 and two locations in the Taupo Zone of New Zealand in late 2021. The results of those trials will be reported in future papers.

REFERENCES

Allis, R., Gwynn, M., Hardwick, C., Kirby, S., Bowers. R., Moore, J., Wannamaker, P., and Simmons, S.: Characteristics of the Cove Fort-Dog Valley-Twin Peaks thermal anomaly, Utah, *Proceedings,* 42nd Workshop on Geothermal Reservoir Engineering, Stanford University, Stanford, CA (2017).

Beardsmore, G.R.: Towards a shallow heat flow probe for mapping thermal anomalies, *Proceedings,* 37th Workshop on Geothermal Reservoir Engineering, Stanford University, Stanford, CA (2012).

Beardsmore, G.R.: Heat flow: the neglected potential field for mineral exploration, *ASEG Extended Abstracts* (2016), 1–6, DOI: 10.1071/ASEG2016ab126.

Beardsmore, G.R. and Antriasian, A.: Developing the 'Heat Needle': a tool for cost effective heat flow mapping. *Proceedings*, World Geothermal Congress 2015, Melbourne, Australia (2015).

Beardsmore, G., Gutiérrez-Negrín, L., Garduño-Monroy, V., Espinoza-Ojeda, O.M., Almanza-Álvarez, S., Antriasian, A., and Egan, S.: Trial Deployment of a surface heat flow probe over the Los Azufres Geothermal Region, Mexico, *Proceedings,* 42nd Workshop on Geothermal Reservoir Engineering, Stanford University, Stanford, CA (2017).

Beardsmore, G., Egan, S., and Sandiford, M.: A Fourier spectral method to measure the thermal diffusivity of soil, *Geotechnical Testing Journal*, **43(3)**, (2020), 20180300. DOI: 10.1520/GTJ20180300.

Carslaw, H.S. and Jaeger, J.C.: *Conduction of Heat in Solids, Second Edition*, Oxford Science Publications, Oxford UK, (1959), 510 pp.

Goldstein, B., Hiriart, G., Bertani, R., Bromley, C., Gutiérrez-Negrín, L., Huenges, E., Muraoka, H., Ragnarsson, A., Tester, J., and Zui, V.: Geothermal Energy, In *IPCC Special Report on Renewable Energy Sources and Climate Change Mitigation* [O. Edenhofer, R. Pichs-Madruga, Y. Sokona, K. Seyboth, P. Matschoss, S. Kadner, T. Zwickel, P. Eickemeier, G. Hansen, S. Schlömer, C. von Stechow (eds)], Cambridge University Press, Cambridge, United Kingdom and New York, NY, USA. (2011).

Hochstein, M.P. and Bromley, C.: Measurement of heat flux from steaming ground, *Geothermics*, 34(2), (2005), 133–160. DOI: 10.1016/j.geothermics.2004.04.002.

Lindsey, C.R., Fairley, J.P., and Larson, P.B.: Dimensional analysis calculation of conductive heat flux in Lower Geyser Basin, Yellowstone National Park, Wyoming, *Proceedings,* 44th Workshop on Geothermal Reservoir Engineering, Stanford University, Stanford, CA (2019).

Magro, G., Bellani, S., and della Vedova, B.: The deep roots of the Larderello Geothermal Field (Italy) from heat flux and ^{3}He anomalies, *GRC Transactions*, **33**, (2009), 405–410.

Mia, M.B., Bromley, C.J., and Fujimitsu, Y.: Heat flux monitoring using satellite based imagery at Karapiti (Craters of the Moon) fumarole area, Taupo, New Zealand, *Proceedings,* 37th Workshop on Geothermal Reservoir Engineering, Stanford University, Stanford, CA (2012).

Minissale, A.: The Larderello geothermal field: a review, *Earth Science Reviews*, **31(2)**, (1991), 133–151. DOI: 10.1016/0012-8252(91)90018-B.

Pollack, H.N., Hurter, S.J., and Johnson, J.R.: Heat flow from the Earth's interior: Analysis of the global data set, *Reviews of Geophysics*, **31(3)**, (1993), 267–280.

Reeves, R., Seward, A., Alcaraz, S., Sanders, F., MacDonald, N., and Brakenrig, T.: Surface heat loss from the Waimangu Geothermal Valley, *Proceedings,* 40th New Zealand Geothermal Workshop, Taupo, New Zealand (2018).

Sacerdoti, A.: Cove Fort—Binary Power Plant, *Proceedings*, World Geothermal Congress 2015, Melbourne, Australia (2015).

Vaughan, R.G., Lowenstern, J.B., Keszthelyi, L.P., Jaworowski, C., and Heasler, H.: Mapping temperature and radiant geothermal heat flux anomalies in the Yellowstone geothermal system using ASTER thermal infrared data, *GRC Transactions*, **36**, (2012), 1403–1410.